An *Ab Initio* Study of the Diadic Prototropic Tautomerism $H_3PX \rightleftharpoons H_2PXH$ ($X = O, NH, CH_2$)

Minh Tho Nguyen and Anthony F. Hegarty*
Department of Chemistry, University College Dublin, Belfield, Dublin 4, Ireland

The diadic prototropic tautomerisms of three model systems $H_3PX \rightleftharpoons H_2PXH$ ($X = O, NH, CH_2$) are investigated by *ab initio* methods. Stationary points corresponding to local minima and transition states are located using gradient techniques at HF/6-31G** level, and relative energies calculated at MP4/6-31G** including a zero-point energy (ZPE) correction, using the optimised geometries. Computation of vibrational frequencies shows a correlation between the norm of the transition-state imaginary frequencies and both the free energy of activation for hydrogen migration and the H_m–P–X angle. The intrinsic barriers $\Delta G_0^{\ddagger}$ calculated by the Marcus theory indicate that all three unimolecular hydrogen transfers belong to a homogenous series. The disparity between the calculated (gas-phase) stabilities and experimental observations based on solution studies is noted. However, it is shown that consideration of the computed net charges dipole moments and electric field gradients of the isolated species, in conjunction with a simple perturbation expression for the solvation energy, allows a successful rationalisation of tautomeric ratios measured in solution.

Owing to the ease with which the phosphorus atom can change its valency from 3 to 4, the diadic prototropic tautomerism (**I**) $\rightleftharpoons$ (**II**) is in some cases a reversible process, the equilibrium position strongly dependent upon the nature of the substituents on both P and X. Although closely related, experimental information about these processes varies. The existence of the methylenephosphorane–alkylphosphine ($X = CR_2$) equilibrium has only recently been established [1] while the alkyl phosphonate–hydroxyphosphine ($X = O$) rearrangement has been known in the chemistry of organophosphorus compounds for nearly 80 years,[2] and the phosphimide–aminophosphine ($X = NR$) interconversion for more than three decades.[3] Recent advances in the chemistry of these tautomerisms involving phosphorus atoms have been described in a comprehensive review by Mastryukova and Kabachink.[4] Although there have been several detailed calculations on the electronic structure and chemical bonding in prototype phosphonium ylides [5] ($X = CH_2$) and phosphine oxides ($X = O$) and their trivalent phosphorus isomers, little is known about the third member of the family, namely the phosphimide (iminophos-λ^5-phane) $H_3P{=}NH$ ($X = NH$). Moreover, in previous studies,[5,6] the interconversion pathway between quadri- and tri-valent isomers have not been fully discussed from the standpoint of the diad prototropic tautomerism. This lack of theoretical information for the $>$PNR system prompts us to consider the rearrangement between model species $H_3P\text{-}NH \rightleftharpoons H_2PNH_2$. In addition, the large difference in the behaviour of P–C, P–N, and P–O compounds with regard to the equilibrium (**I**) $\rightleftharpoons$ (**II**) in solution suggests the need for a comparative study of the interconversions of these systems. The main purpose of the present study is thus to compare the unimolecular 1,2-hydrogen shifts connecting the prototype (**I**) and (**II**) species by performing calculations at the same high level of accuracy.

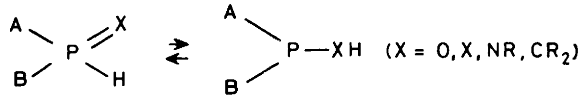

(**I**) (**II**)

Calculations

All calculations were performed using the Gaussian-81 [7] program and two basis sets: 3-21G* (including only six cartesian *d*-functions on P) [8] and 6-31G* (including polarisation *d*-functions on C, N, O, and P and *p*-functions on H).[9] The relative energies of the stationary points of each system were estimated using Møller–Plesset perturbation theory to fourth-order, including all single, double, and quadruple excitations (MP4SDQ)[10] at the 3-21G*-optimized geometries with the HF/6-31G** wavefunctions as references for generating excited configurations. Harmonic vibrational frequencies were computed with the 3-21G* basis making use of the analytic second derivatives. The best estimation for the energy differences between stationary points thus includes MP4SDQ/6-31G** values plus zero-point energy contributions.

Results and Discussion

(1) *The Phosphine Oxide–Phosphinous Acid Tautomerism.*— The pathway of the reaction $H_3PO \rightleftharpoons H_2POH$ has previously been studied in some detail by Schmidt *et al.*[6] These authors reported the optimised geometries of three stationary points (the two local minima and the transition state for 1,2-shift connecting them) with the 3-21G* basis set, and the energy differences between them at the MP3/6-31G* level. An energy-localised orbital analysis has also been described.

Table 1 contains total and relative energies and some thermochemical properties of H_3PO (**1**), H_2POH (**3**), and the transition structure (TS) (**2**) calculated at different levels. Thermochemical properties relating to the gas-phase rearrangement are listed in Table 2.

Although the HF/3-21G* energies obtained for these species in the present work are lower (0.06 a.u.) than those reported in ref. 6, calculated using five spherical harmonic *d*-orbitals on phosphorus, their optimised geometrical parameters are similar, and are not shown here. The TS (**2**) possesses C_s symmetry; the migration of hydrogen occurs in the molecular plane. To see more clearly the type of motion involved in each normal mode during the transformation, harmonic vibrational frequencies are drawn as a correlation diagram in Figure 1. At

Table 1. Total (a.u.), relative (in parentheses, kcal mol^{-1}), and zero-point vibrational (ZPE/kcal mol^{-1}) energies, entropies (S/cal mol^{-1} K^{-1}), and specific heat capacity (C_p/cal mol^{-1} K^{-1}) for three stationary points on the H_3PO energy surface[a]

	H_3PO (**1**) (C_{3v})	TS (**2**) (C_s)	H_2POH (**3**) (C_s)
HF/3-21G*[b]	−415.266 04 (6.1)	−415.128 18 (92.6)	−415.275 76 (0.0)
HF/6-31G**	−415.313 04 (7.1)	−417.184 00 (88.1)	−417.324 33 (0.0)
MP4SDQ/6-31G**	−417.641 86 (5.0)	−417.535 45 (71.8)	−417.649 86 (0.0)
ZPE	21.6	18.0	21.2
S_2 (298.15 K)	57.8	58.4	59.7
C_p (298.15 K)	9.4	10.4	11.2

[a] Using the 3-21G* optimised geometry. [b] The HF/3-21G* energies reported in ref. 6: (**1**) −415.207 01; (**2**) −415.068 22; and (**3**) −415.216 65 a.u.

Table 2. Thermochemical properties of the gas-phase H_3PO (**1**) $\longrightarrow$ H_2POH (**3**) rearrangement

Property[a]		Estimated value
Heat of reaction (kcal mol^{-1})	ΔH°_{13} (0 K)	−5.4
	ΔH_{13} (298.15 K)	−4.9
Entropy of reaction (cal mol^{-1} K^{-1})	ΔS_{13} (298.15 K)	1.9
Free energy of reaction (kcal mol^{-1})	ΔG_{13} (298.15 K)	−5.5
Energy barrier (kcal mol^{-1})	$\Delta H^\ddagger_{13}$ (0 K)	63.2
	$\Delta H^\ddagger_{13}$ (298.15 K)	63.5
Activation entropy (cal mol^{-1} K^{-1})	$\Delta S^\ddagger_{13}$ (298.15 K)	0.6
Free energy of activation (kcal mol^{-1})	$\Delta G^\ddagger_{13}$ (298.15 K)	63.3

[a] ΔH (0 K) = ΔE (MP4) − ΔZPE. ΔH (298.15 K) = ΔH (0 K) + $\int \Delta C_p dt$. $\Delta S_{12} = S_2 - S_1$. $\Delta G = \Delta H - T\Delta S$.

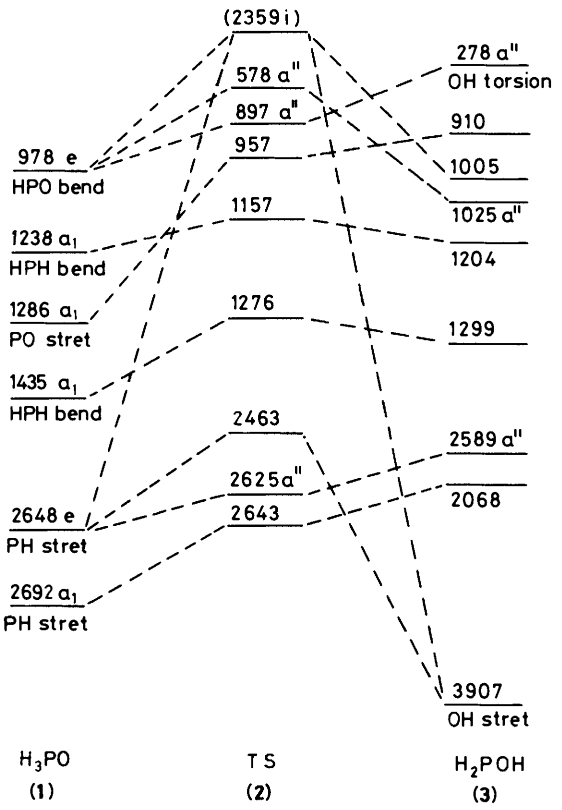

Figure 1. Vibrational frequencies correlation diagram for the [H_3PO] stationary points (3-21G*). Values are given in cm^{-1} and the scale is arbitrary

the TS (**2**), there is an overall shift to lower frequencies with respect to those in H_3PO. The stretching frequency in the TS is calculated to lie nearer to that of H_2POH although the bending modes are more affected than the PH (non migrating) stretchings.

In particular, the imaginary frequency of 2359i cm^{-1} describing the migration of the hydrogen atom is due to a combination of both PH_m (1.448 Å) bond length and H_mPO (56.7°) bond angle co-ordinates.

The relative energies of the stationary points computed at MP3/6-31G* in the previous work[6] [(**3**) (0 kcal mol^{-1}) < (**1**) (5.6) < (**2**) (75.6)] are similar to the present MP4SDQ/6-31G** values (Table 1), although the activated complex is stabilised by an increase in the correlation energy. As expected for this type of unimolecular rearrangement, the variation of entropy (Table 2) is very small so that the gas-phase reaction (**1**) $\longrightarrow$ (**3**) is totally controlled by the enthalpy of activation. The final estimation predicts reaction to be slightly exothermic (ΔG_{13} −5.5 kcal mol^{-1}) with a substantial free energy of activation ($\Delta G^\ddagger_{13}$ 63.3 kcal mol^{-1}).

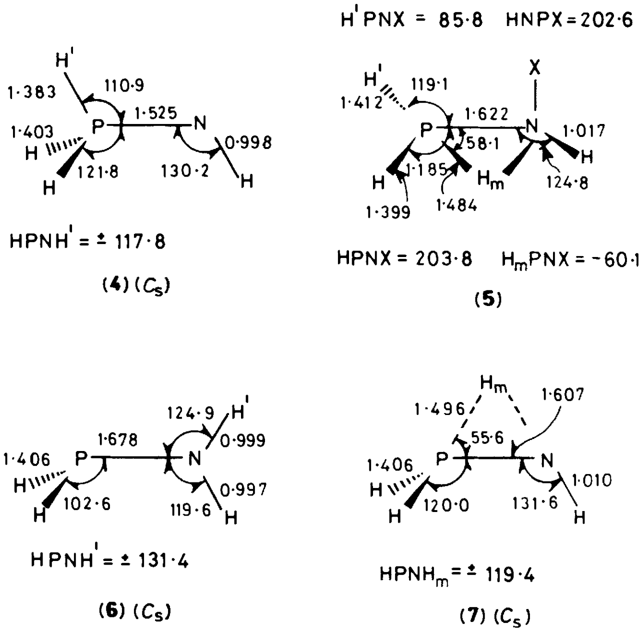

Figure 2. HF/3-21G* geometries of four stationary points on the [H_4PN] energy surfaces. Bond lengths in Å and bond angles in degrees

(2) *The Phosphimide–Aminophosphine Tautomerism.*—The optimised geometries of the stationary points H_3PNH (**4**), $H_2P(H)NH$ (**5**) and (**7**), and H_2PNH_2 (**6**) are displayed in Figure 2 and the calculated energetic and thermodynamic parameters are summarised in Tables 3 and 4. Computed harmonic vibrational frequencies are shown in Figure 3.

Independent of the level of calculations, aminophosphine is more stable than the H_3PNH (**4**) isomer. The free energy of reaction amounts to ΔG_{46} −31.8 kcal mol^{-1}. As a consequence,

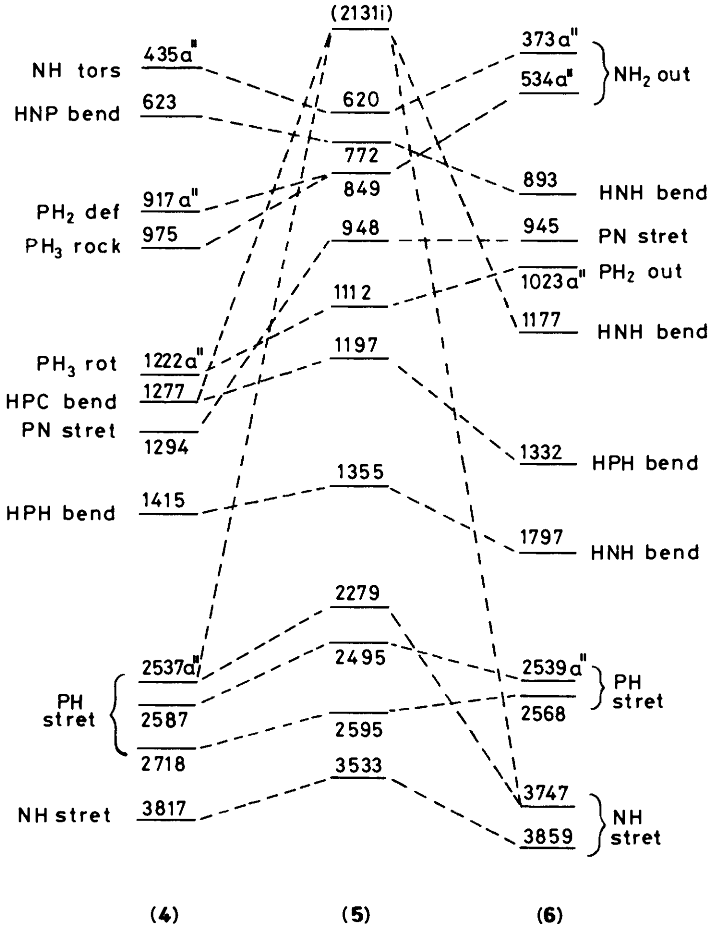

Figure 3. Vibrational frequencies correlation diagram for three $[H_4PN]$ stationary points. Values are in cm^{-1} and the scale is arbitrary

Table 3. Total (a.u.), relative (in parentheses, kcal mol^{-1}) and zero-point vibrational (ZPE/kcal mol^{-1}) energies, entropies (S/cal mol^{-1} K^{-1}), and specific heat capacities (C_p/cal mol^{-1} K^{-1}) for four stationary points on the $[H_4PN]$ energy surface

	H_3P–NH (**4**)	$H_2P(H)NH$ (**5**)	H_2P–NH_2 (**6**)	$H_2P(H)NH$ (**7**)
HF/3-21G*	−395.491 70 (40.8)	−395.378 39 (111.9)	−395.556 69 (0.0)	−395.376 06 (113.3)
HF/6-31G**	−397.436 40 (35.5)	−397.328 39 (103.3)	−397.492 96 (0.0)	−397.324 72 (105.5)
MP4SDQ/6-31G**	−397.761 02 (33.4)	−397.674 06 (88.0)	−397.814 34 (0.0)	−397.667 31 (92.2)
ZPE	28.3	25.4	29.7	24.5
S (298.15 K)	59.2	58.9	60.0	58.5
C_p (298.15 K)	11.8	11.3	12.3	10.3

Table 4. Thermochemical properties of the gas-phase H_3PNH (**4**) ⟶ H_2PNH_2 (**6**) rearrangement

Property[a]		Estimated value
Heat of reaction (kcal mol^{-1})	ΔH°_{46} (0 K)	−32.0
	ΔH_{46} (298.15 K)	−31.6
Entropy of reaction (cal mol^{-1} K^{-1})	ΔS_{46} (298.15 K)	0.8
Free energy of reaction (kcal mol^{-1})	ΔG_{46} (298.15 K)	−31.8
Energy barrier (kcal mol^{-1})	$\Delta H^\ddagger_{46}$ (0 K)	51.7
	$\Delta H^\ddagger_{46}$ (298.15 K)	51.6
Activation entropy (cal mol^{-1} K^{-1})	$\Delta S^\ddagger_{46}$ (298.15 K)	−0.3
Free energy of activation (kcal mol^{-1})	$\Delta G^\ddagger_{46}$ (298.15 K)	51.7

[a] See footnote in Table 2 for definitions.

the activation energy becomes smaller than that in the H_3PO case. In fact, the free energy of activation for the gas-phase rearrangement (**4**) ⟶ (**6**) *via* the TS (**5**) is estimated at 51.7 kcal mol^{-1}. The activation entropy is negative in this reaction but its absolute value is negligible (see Table 4).

The geometry of aminophosphine (**6**) has been studied in some previous papers.[11,12] Owing to the lack of polarisation functions on nitrogen atom in the 3-21G* basis set, the amino group is found to be planar. Nevertheless, the energy difference between the planar and pyramidal forms has been shown to be extremely small (0.2 kcal mol^{-1}).[10]

The P–N bond length in the non-classical H_3PNH (**4**) (1.525 Å) is much shorter than that in H_2PNH_2 (1.678 Å), but close to the experimental (X-ray) value of 1.536 Å determined for a substituted $>$P–N– compound.[13] It is noted that in this

Table 5. Total (a.u.), relative (in parentheses, kcal mol^{-1}) and zero-point vibrational (ZPE/kcal mol^{-1}) energies, entropies (*S*/cal mol^{-1} K^{-1}), and specific heat capacities (C_p/cal mol^{-1} K^{-1}) for four stationary points on the [H_5PC] energy surface

	H_3P-CH_2 (**8**)	$H_2P(H)CH_2$ (**11**)	H_2PCH_3 (**10**)	$H_2P(H)CH_2$ (**9**)
HF/3-21G*	−379.549 37 (57.6)	−379.431 34 (131.6)	−379.641 09 (0.0)	379.467 05 (109.2)
HF/6-31G**	−381.402 12 (58.5)	−381.292 97 (127.0)	−381.495 38 (0.0)	−381.323 07 (108.1)
MP4SDQ/6-31G**	−381.706 98 (58.7)	−381.611 15 (118.8)	−381.800 42 (0.0)	−381.650 73 (94.0)
ZPE (298.15 K)	35.1	31.3	36.9	33.4
S (298.15 K)	61.1	59.9	61.1	59.5
C_p (298.15 K)	43.2	12.0	11.6	11.8

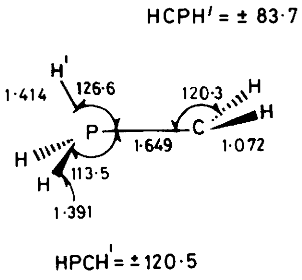

(**8**) (C_s)

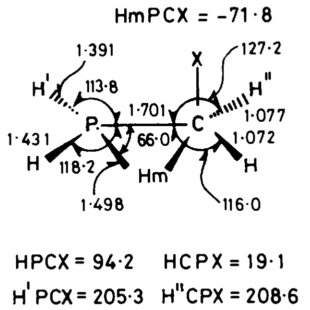

(**9**)

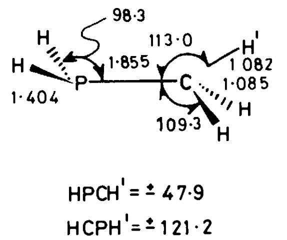

(**10**) (C_s)

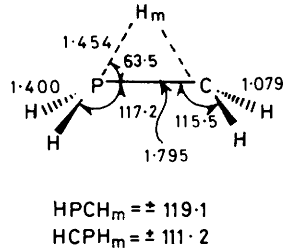

(**11**) (C_s)

Figure 4. HF/3-21G* geometries of four stationary points on the [H_5CP] energy surfaces. Bond lengths in Å and bond angles in degrees

Table 6. The predicted thermochemical data for the gas-phase H_3P-CH_2 (**8**) $\longrightarrow$ H_2P-CH_3 (**10**) rearrangement

	Parameters[a]	Predicted value
Heat of reaction	ΔH°_{810} (0 K)	−56.9
	ΔH_{810} (298.15 K)	−57.4
Entropy of reaction	ΔS_{810} 298.15 K)	0.0
Free energy of reaction	ΔG_{810} (298.15 K)	−57.4
Energy barrier	$\Delta H^\ddagger_{810}$ (0 K)	33.6
	$\Delta H^\ddagger_{810}$ (298.15 K)	33.2
Activation entropy	$\Delta S^\ddagger_{810}$ (298.15 K)	−1.6
Free energy of activation	$\Delta G^\ddagger_{810}$ (298.15 K)	33.7

[a] See Table 1 for definition and units.

crystal structure the phosphorus atom has a nearly planar conformation whereas the group in (**4**) is strongly 'pyramidal'. The calculated P–N stretching frequency of 1 294 cm^{-1} in (**4**) also ranges within the i.r. values of 1 100—1 495 cm^{-1} observed for a large number of phosphimide compounds.[14] It seems that this frequency is quite sensitive to substituent effects, in particular by π-donor groups on the phosphorus atom. Such a frequency is close to that of the typical double bond of (1 250 cm^{-1}) in iminophosphane (–P=N–).[15]

As in the $H_3PO \rightleftharpoons H_2POH$ tautomerism, the PN stretching frequency in the transition state (**5**) is quite close to that of the product (**6**). The variation of the remaining normal modes also follows the pattern discussed for the phosphine-oxide tautomerism. The imaginary frequency corresponding to the hydrogen shift is at 2 131i cm^{-1}, slightly smaller than the $H_2P(H)O$ value of 2 359i. Structure (**7**), which possesses C_s symmetry, exhibits two imaginary frequencies. The first of them 2 379i is somewhat higher than the corresponding value in (**5**), whereas the second frequency of 515i cm^{-1} involves the out-of-plane movement of the migrating hydrogen.* The energy difference between the two maxima is small [$\Delta(\Delta H_{298.15})$ 3 kcal mol^{-1}]. This reflects the fact that the energy surface is extremely flat along the rotation of the P–H_m group around the P–N bond. From a technical point of view, only the use of analytical energy second derivatives in the optimisation allows an unambiguous location of the true transition state. With regard to the preference of the non-symmetrical migration *via* (**5**) over the symmetrical one *via* (**7**), we refer to a detailed examination in an earlier paper.[15]

(3) *The Methylenephosphorane–Methylphosphine Tautomerism.*—The geometry of four stationary points (**8**)—(**11**) on the CH_5P energy surface are shown in Figure 4. The computed energetic and thermochemical data are listed in Tables 5 and 6, respectively. Harmonic vibrational frequencies are collected in Figure 5.

The electronic and structural aspects of both potential minima methylphosphorane (**8**) and methylphosphine (**10**) have been discussed by a number of authors.[16–18] The present 3-21G*-optimised geometries (Figure 4) are similar to earlier data (see ref. 18 for instance). The ΔH° (0 K) values estimated at MP3/6-1G** level in ref. 6 differ only slightly from the MP4SDQ/6-31G** data shown in Table 6.

For the conversion (**8**) $\longrightarrow$ (**10**), *via* the TS (**9**), our calculation predicts ΔG(298.15 K) −57.4 and $\Delta G^\ddagger$ (298.15 K) 33.7 kcal mol^{-1} for the free energies of reaction and activation, respectively.

As seen in Figure 5, the P–C and P–H bonding of the phospholium ylide (**8**) vibrate at 1 060 and 2 542—2 674 cm^{-1}, respectively (3-21G*). These theoretical values are comparable with the experimental ones of 1 078—1 085 and 2 360—2 400 cm^{-1} obtained from i.r. spectra of a few substituted P–H ylides.[19] It is well established that the 3-21G* frequency for the PH stretching mode is overestimated by *ca.* 10%,[20] but the situation for the P–C bond is not so clearcut. Like the previous case (P–N) the latter appears to be highly susceptible to the presence of substituents. For example, the present P–C frequency of 1 060 cm^{-1} is markedly smaller than that of 1 428 cm^{-1} previously calculated with a DZP basis set for the phospholium cyclopropyl ylide $H_3P{=}C(CH_2)_2$.[21]

---

* The remaining vibrational frequencies of structure (**7**) are (3-21G*) 3 610, 2 562, 2 533 (a″), 2 304, 1 337, 1 208, 1 054, 933, 843 (a″), and 786 cm (a″).

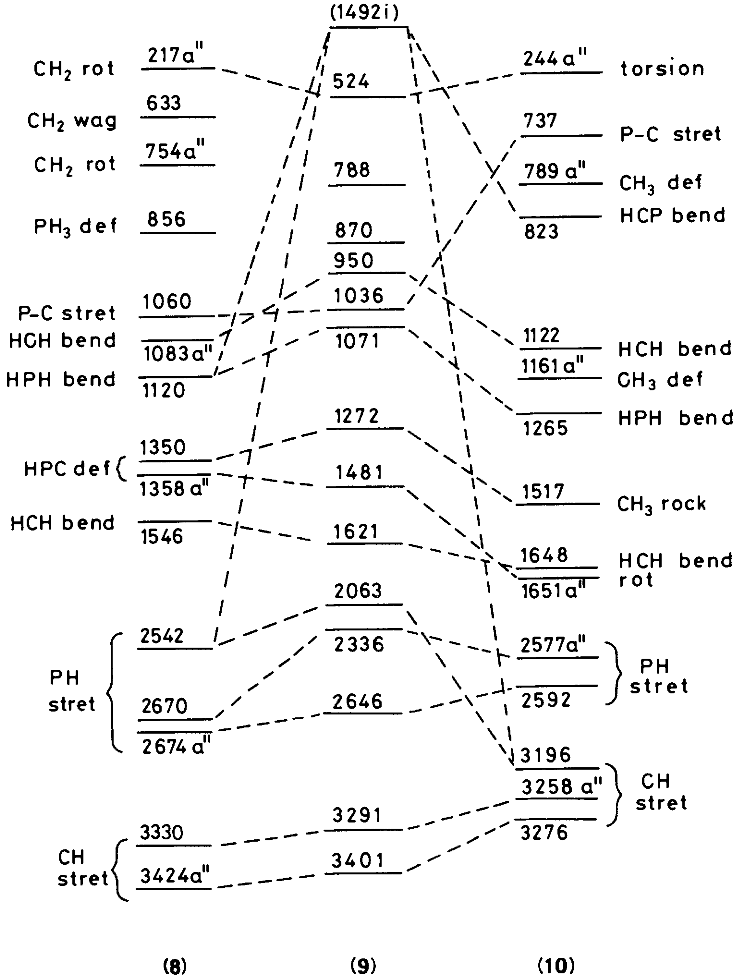

Figure 5. Correlation diagram of the harmonic vibrational frequencies (cm^{-1}) for three stationary points on the $H_3PCH_2 \longrightarrow H_2P\text{–}CH_3$ rearrangement pathway. The scale is arbitrary

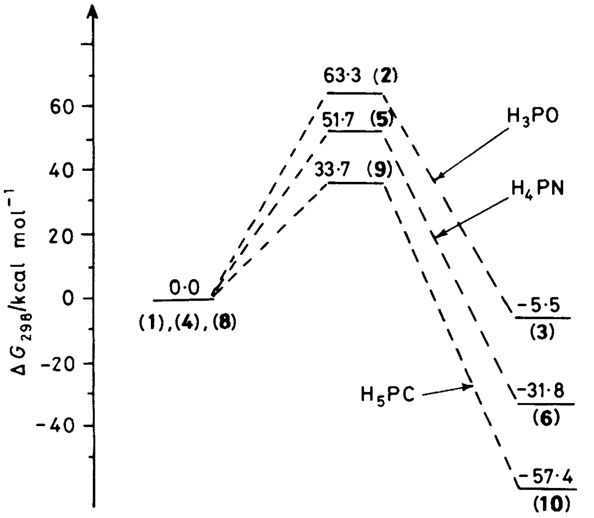

Figure 6. Energy profiles of three diadic prototropic tautomerisms $H_3PX \longrightarrow H_2PXH$

It is worth noting that unlike the $H_2P(H)C$ and $H_2P(H)NH$ transition states, the PC stretching frequency in the TS (**9**) (1 036 cm^{-1}, Figure 5) is much closer to that in the ylide form (**8**) (1 060 cm^{-1}) than to that in the phosphine form (**10**) (737 cm^{-1}). In addition, the imaginary frequency 1 492i in (**8**) is also significantly smaller than those of 2 359i in H_3PO (**3**) and 2 131i in H_2PNH (**5**). This is no doubt a reflection in the vibrational parameters, of the increased exothermicity of the rearrangement H_3PCH_2 (**8**) $\longrightarrow$ (H_2PCH_3) (**10**) with respect to the earlier ones. The planar stationary point (**11**) has two imaginary frequencies of 3 156i and 786i cm^{-1}. Both are large in comparison with the corresponding values in (**9**) (1 492i for the former) and in (**7**) (515i for the latter). Moreover, the energy difference between both maxima (**9**) and (**11**) is substantial (22.7 kcal mol^{-1} at MP4 and ZPE, Table 5). Although the energy surfaces in the immediate neighbourhood of the oxide point (**9**) is also very flat along the co-ordinate describing the rotation of the migrating hydrogen around P–C bond, a difference of this magnitude indicates on the one hand a clear preference for the non-symmetrical pathway over the symmetrical one and, on the other hand, the strong energetic compensation provided by the avoided repulsion between two migrating lone pairs [the π(PH) and the carbon lone pair] for the disfavoured geometrical conformation of the TS (**9**).

(4) *Summary and Comparison with Experiment.*—The free energy profiles of the unimolecular prototropic tautomerisms considered are shown schematically in Figure 6. It is seen that the exothermicity of the reactions is appreciably increased in the sequence $H_3PO \longrightarrow H_3PNH \longrightarrow H_3PCH_2$. The successive replacement of O by NH and NH by CH_2 thus increases the PH

acidity and stabilises the trivalent phosphine form by approximately the same amount (a free energy change of *ca.* 26 kcal mol^{-1}). Conversely, the free energy of activation decreases more rapidly in going from H_3PNH to H_3PCH_2 (18 kcal mol^{-1}) than from H_3PO to H_3PNH (11.6 kcal mol^{-1}). This is in line with considerations based on Marcus' theory,[22] which relates the free energy of activation ($\Delta G^\ddagger$) to the free energy of the reaction (ΔG) by relationship (1)[23] where $\Delta G^\ddagger$ represents the

$$\Delta G^\ddagger = \Delta G_0^\ddagger\left(1 + \frac{\Delta G}{4\Delta G_0^\ddagger}\right)^2 \tag{1}$$

'intrinsic barrier' ($\Delta G_0^\ddagger = \Delta G^\ddagger$ when $\Delta G = 0$). Regarding the three 1,2-shift studies as a series of homogenous reactions, we can now introduce the Brønsted exponent α which is defined by differentiating equation (1) leading to (2). Employing energetic

$$\alpha = \frac{d\Delta G^\ddagger}{d\Delta G} = \tfrac{1}{2}\left(1 + \frac{\Delta G}{4\Delta G_0^\ddagger}\right) \tag{2}$$

data given in Figure 6 with the aid of equations (1) and (2), the kinetic parameters α and $\Delta G_0^\ddagger$ for each rearrangement were calculated and are listed in Table 7.

The calculated intrinsic barrier is found to be nearly the same in each case and amounts to $\Delta G_0^\ddagger$ 63 ± 4 kcal mol^{-1}. This supports the hypothesis that all three 1,2-hydrogen-transfer reactions belong to a homogenous series.

It is well recognised that the norm of the imaginary frequency in the transition state (ν_i) indicates the height of the activation barrier. According to More O'Ferrall,[24] this is also a measure of the transfer angle during a proton-transfer process. Indeed, Figure 7 shows a parabolic relationship between ν_i and $\Delta G^\ddagger$ and a quasi-linear relationship between ν_i and the bond angle $\beta = H_mPX$ (H_m = transferred hydrogen, X = O, N, and C). It is interesting that an inverse relationship $\beta = f(\nu_i)$ has been found for the 1,5-hydrogen shift.[25]

Table 7. Bond order at transition state (n_{TS}), Brønsted exponent (α), and intrinsic barrier ($\Delta G_0^\ddagger$) of three rearrangements

Reaction	α	$\Delta G_0^\ddagger$/kcal mol^{-1}
$H_3PO \longrightarrow H_2POH$	0.49	66.0
$H_3PNH \longrightarrow H_2PNH_2$	0.44	66.7
$H_3PCH_2 \longrightarrow H_2PCH_3$	0.39	58.9

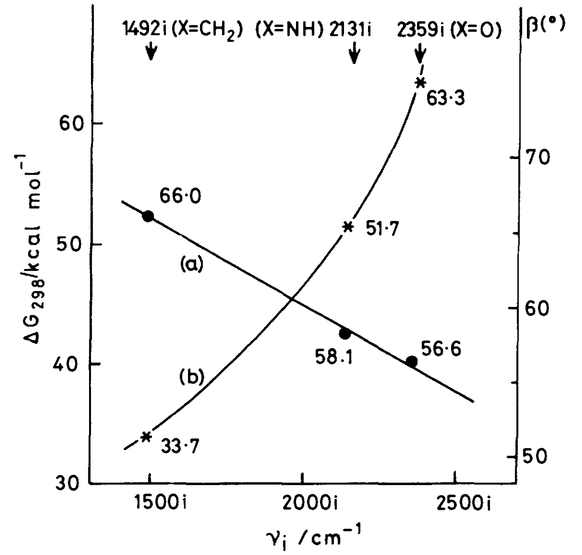

Figure 7. Correlation between the imaginary frequency ν_i (cm^{-1}) and (a) the free energy of activation ($\Delta G^\ddagger$) and (b) bond angle H_m-P-X (β) for three $H_3PX \rightleftharpoons H_2PXH$ rearrangements

It is important to remember that the above discussion is only valid for the tautomerism process under ideal gas conditions. We now attempt to use these results to understand experimental findings for reactions occurring in solution.

Consider first the oxygen diad. As seen in Figure 6, both H_3PO and H_2POH species are quite stable in the gas phase with respect to the hydrogen migration. In contrast, the tautomeric equilibrium in solution has been found to be completely displaced towards the tetra-co-ordinated phosphorus ABPH-O isomer. Proof of the existence of the hydroxy form (ABP-OH) has been obtained in the case where A and B are strong σ-captor (such as CF_3)[26] or π-donor (OR or SR)[27] groups. Thus it is clear that the oxygen diadic tautomerism is crucially dependent upon substituents and solvent effects, which both favour the P–H isomer over the O–H.

Table 8 shows the positive net charge on the phosphorus atom is substantially reduced in the activated complex (**2**), while the atomic charge on the migrating hydrogen becomes markedly positive. Thus, the polarity of the PH bond (P^+–H^-) is significantly decreased in going from H_3PO (**1**) to the transition state (**2**) (P^+–H^+). This view is supported by the computed electric field gradients of the hydrogen (Table 8). The q_{zz} components indicate the relative ionic character of chemical bonds. Possessing a large q_{zz} value, the H_m atom in (**3**) is hence more positive than that in (**1**) and (**2**). Although the polarity of the PH and OH bonds cannot be directly compared, both the net charge and in particular the q_{zz} value seem to indicate that the H(O) atom in (**3**) is much more acidic than the H(P) in (**1**). As a consequence, the hydrogen shift could become more difficult to achieve in the direction (**1**) $\longrightarrow$ (**3**), than that in the opposite direction (**3**) $\longrightarrow$ (**1**). Introduction of σ-captor substituents appears to enlarge the positive net charge on the H_m atoms in (**2**), whereas π-donor groups reduce the positive net charge of the P atom. Both actions create a similar effect by rendering the H_m atom more labile and hence favouring the formation of the hydroxy form (**3**).

In addition, the large dipole moment of (**1**) (Table 8) suggests that this species is even more strongly favoured by polar solvents at the expense of (**3**). We can estimate the solvation

$$SE = A.\frac{\sum_i C_{iL}^2}{\varepsilon_L - \varepsilon_H} \tag{3}$$

energies (SEs) in a simple way *via* relationship (3)[28–30] where A is a proportionality constant, C_{iL} the LUMO coefficients, and ε_L and ε_H the energies of the LUMO and HOMOs, respectively. In the present case, the SE arises from the stabilising charge-

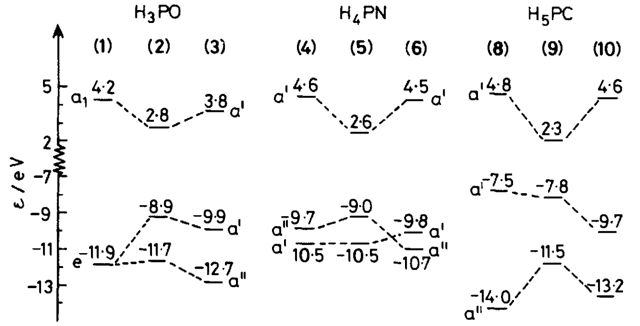

Figure 8. Frontier orbital energies (eV) of each stationary point on the $H_3PX \rightleftharpoons H_2PXH$ pathways

Table 8. Molecular properties of stationary points calculated at HF/6-31G** level

Property	$H_3PO \rightleftharpoons H_2POH$			$H_3PNH \rightleftharpoons H_2PNH_2$			$H_3PCH_2 \rightleftharpoons H_2PCH_3$		
	(1)	**(2)**	**(3)**	**(4)**	**(5)**	**(6)**	**(8)**	**(9)**	**(10)**
Net charge: P	1.05	0.65	0.57	0.91	0.55	0.47	0.70	0.40	0.30
X^a	−0.72	−0.77	−0.75	−0.86	−0.85	0.88	−0.70	−0.58	−0.57
$H_m{}^b$	−0.11	0.31	0.37	−0.13	0.25	0.30	−0.06	+0.06	0.15
H(P)	−0.11	−0.09	−0.10	−0.07	0.11	−0.10	−0.14	−0.10	−0.07
H(X)				0.29	0.26	0.29	0.13	0.14	0.14
Dipole moment μ^c	4.2	3.4	1.5	2.9	2.3	1.61	2.4	0.42	1.37
Overlap population P=X^a	1.10	0.25	0.42	1.24	0.26	0.54	1.24	0.70	0.60
Electric field gradient^d $^q xx(H_m)$	−0.09	−0.17	−0.21	−0.09	−0.14	−0.27	−0.09	−0.11	−0.16
$^q yy(H_m)$	−0.09	−0.05	−0.26	−0.10	−0.04	−0.18	−0.08	−0.04	−0.15
$^q zz(H_m)$	0.18	0.22	0.47	0.19	0.18	0.45	0.17	0.15	0.31

^{a} X = O, N and CH_2, respectively. ^{b} Migrating hydrogen. ^{c} In Debye units. ^{d} In principal axis systems, a.u.

transfer interaction between the HOMOs of the phosphorus species and the LUMOs of electron-captor (protic, for example) solvent molecules.

According to the HOMO energies given in Figure 8, equation (3) predicts an increasing order of SEs as follows: TS(2) > H_2POH (3) > H_3PO (1). This means that protic solvents might favour the formation of the phosphine form (3).

To summarise, the charge distribution data in the model species (1)—(3) of the oxygen diadic tautomeric pathways allow us to understand the trends observed in solution. For the nitrogen diad ABPH–NR $\rightleftharpoons$ ABP–NHR, where A, B, and R are alkyl, aryl, or alkoxy groups, the tautomeric equilibria were found to be displaced under different solution conditions towards the formation of the trivalent phosphine form (ABP–NHR). Unlike the oxygen diad, PH isomers can be detected for a large number of P–N compounds, however. Equilibria involving both PH and NH forms are also frequently observed. Considering the carbon diad ABPH–CR^1R^2 $\rightleftharpoons$ ABP–CHR^1R^2, the tautomerism is quite reversible; the equilibrium position depending on the nature of the solvent, concentration, temperature, and substituents at the P atoms.[21] From Table 8, we note that the charge distribution in both the nitrogen or carbon diad systems (4)—(6) and (8)—(10) presents many similarities to that in oxygen diad discussed above. This implies that a similar substituents effect also exists for both the PN and PC rearrangements.

Actually, strong σ-captor or π-donor substituents attached on one centre always favours the migration of a hydrogen to the adjacent centre.[4] In particular, the predominance of the phosphine forms in the absence of solvent[19] (*i.e.* in the pure liquids) can also be understood by the increasing exothermicity and the decreasing free energy of activation of the rearrangement, which favours them (Figure 6). On the other hand, Kolodiazhnyi[19] showed that the ratio of PH and CH forms in the carbon diadic tautomerism of a given P–C compound varies from 10:90 in the presence of cyclohexane solvent to 61:39 in chloroform. This correlates well with the larger dipole moment in all of the PH forms, in comparison with their XH isomers (Table 8). In addition, according to the HOMO energies displayed in Figure 8 and equation (3), the opposite trend to that in the oxygen diad appears to be observed for both nitrogen and carbon diads. In a protic solution (such as chloroform) the solvation energy due to the PH form, is larger than that of the XH form and consequently the solvated PH compounds become favoured over the solvated XH. This argument, which is based on a very simple perturbation approach [equation (3)] can thus endorse the solvent effect as stated above.

In conclusion, we present in this work an *ab initio* study on the prototropic tautomerisms of three simple model diads. The behaviour of species considered in the gas phase appears to be quite different from that observed in solution. Nevertheless, a detailed analysis of calculated data yields a better understanding of these transformations which have been investigated experimentally over the past several decades, and provides in the same occasion a reasonable theoretical support for interpretations based on experimental findings.[4]

Acknowledgements

We are indebted to the Department of Education (Irish Government) for financial support. We also thank the U.C.D. Computer Centre for a computer-time grant. Dr. M. McGinn is gratefully acknowledged for assistance.

References

1 T. A. Mastryukova, I. M. Aladzheva, I. V. Leont'eva, V. A. Svoren, P. V. Petrovskii, and M. I. Kabachnik, *Zh. Obshch. Khim.*, 1972, **42**, 2454.

2 A. E. Arbuzov, *Izv. Akad. Nauk. SSSR*, 1952, 41.

3 M. I. Kabachnik and V. A. Gilyarov, *Dokl. Akad. Nauk SSSR*, 1954, **96**, 91.

4 T. A. Matryukova and M. I. Kabachnik, *Usp. Khim.*, 1983, **52**, 1761.

5 M. W. Schmidt, S. Yabushita, and M. S. Gordon, *J. Phys. Chem.*, 1984, **88**, 382.

6 B. F. Yates, W. J. Bouma, and L. Radom, *J. Am. Chem. Soc.*, 1984, **106**, 5805, and references therein.

7 J. S. Binkley, M. J. Frisch, D. J. DeFrees, K. Raghavachari, R. A. Whiteside, H. B. Schlegel, E. Fluder, and J. A. Pople, Program Gaussian-82, Carnegie-Mellon University.

8 M. S. Gordon, J. S. Binkley, J. A. Pople, W. J. Pietro, and W. J. Hehre, *J. Am. Chem. Soc.*, 1982, **104**, 2792, and references therein.

9 P. C. Hariharan and J. A. Pople, *Theor. Chim. Acta*, 1973, **28**, 213.

10 R. Krishnan and J. A. Pople, *Int. J. Quant. Chem.*, 1978, **14**, 91.

11 D. Gonbean, D. Liotard, and G. Pfister-Guillouzo, *Nouv. J. Chim.*, 1980, **4**, 227.

12 M. Barthelat, R. Mathis, and F. Mathis, *J. Mol. Struct.*, 1981, **83**, 351.

13 M. R. Marre, M. Sandez, R. Wolf, J. Jaud, and J. Galy, *Can. J. Chem.*, 1984, **62**, 2186.

14 Yu. P. Egorov and A. A. Kudryavtsev, *Zh. Obshch. Khim.*, 1983, **53**, 2222.

15 M. T. Nguyen, M. A. McGinn, and A. F. Hegarty, *J. Am. Chem. Soc.*, 1985, **107**, 8029.

16 H. Lischka, *J. Am. Chem. Soc.*, 1977, **99**, 354.

17 D. J. Mitchell, S. Wolfe, and H. B. Schlegel, *Can. J. Chem.*, 1981, **59**, 3280.

18 D. A. Dixon, T. H. Dunning, R. A. Eades, and P. G. Grassmann, *J. Am. Chem. Soc.*, 1983, **105**, 7011.

19 O. I. Kolodiazhny, *Tetrahedron Lett.*, 1980, **21**, 2269.

20 M. T. Nguyen, A. F. Hegarty, T. K. Ha, and P. Brint, *Chem. Phys.*, 1985, **98**, 447.

21 M. Vincent, H. F. Schaefer, P. Schier, and H. Schmidbaur, *J. Am. Chem. Soc.*, 1983, **105**, 3806.
22 R. A. Marcus, *Faraday Symp. Chem. Soc.*, 1975, **10**, 60 and references therein.
23 N. Agmon, *J. Chem. Soc., Faraday Trans. 2*, 1978, **74**, 388.
24 R. A. More O'Ferrall, *J. Chem. Soc., Perkin Trans. 2*, 1970, 785.
25 N. G. Rondan and K. N. Houk, *Tetrahedron Lett.*, 1984, **25**, 2519.
26 J. E. Griffith and A. B. Burg, *J. Am. Chem. Soc.*, 1962, **84**, 3442.
27 E. E. Nifant'ev and I. V. Shilov, *Zh. Obshch. Khim.*, 1972, **42**, 1936.
28 M. J. S. Dewar and R. C. Dougherty, 'The PMO Theory of Organic Chemistry,' Plenum Press, New York, 1975.
29 W. L. Jorgensen, *J. Am. Chem. Soc.*, 1977, **99**, 200.
30 D. Cremer, J. Gauss, R. F. Childs, and C. Blackburn, *J. Am. Chem. Soc.*, 1985, **107**, 2435.

Received 13*th January* 1986; *Paper* 6/097